ChemPubSoc Europe
DOI: 10.1002/chem.201404662
CHEMISTRY
A European Journal
Full Paper

Synthetic Carbon Allotropes

Novel λ^3-Iodane-Based Functionalization of Synthetic Carbon Allotropes (SCAs)—Common Concepts and Quantification of the Degree of Addition

Ferdinand Hof, Ricarda A. Schäfer, Cornelius Weiss, Frank Hauke, and Andreas Hirsch*[a]

Abstract: The covalent functionalization of carbon allotropes represents a main topic in the growing field of nano materials. However, the development of functional architectures is impeded by the intrinsic polydispersibility of the respective starting material, the unequivocal characterization of the introduced functional moieties, and the exact determination of the degree of functionalization. Based on a novel carbon allotrope functionalization reaction, utilizing λ^3-iodanes as radical precursor systems, we were able to demonstrate the feasibility to separate and to quantify thermally detached functional groups, formerly covalently linked to carbon nanotubes and graphene through thermogravimetric GC-MS.

Introduction

Inspired by the rich chemistry of fullerenes, the functionalization of other synthetic carbon allotropes (SCAs), in particular carbon nanotubes and more recently graphene, has steadily been progressed.[1] In parallel to the development of efficient reaction protocols, such as the reductive alkylation and arylation of SCAs,[2] tools for product characterization have continuously been adjusted and improved.[3] Typical techniques are: thermogravimetric analysis,[4] Raman spectroscopy,[3g] STM/AFM,[5] and XPS.[6] However, the powerful analytical tool-kit, routinely used for the structural characterization of organic molecules, such as NMR spectroscopy, mass spectrometry, and X-ray crystallography can hardly be applied for the analysis of covalently functionalized carbon nanotubes and graphene, due to their intrinsic polydisperse nature. Here, only mixtures of adducts with a broad distribution of sizes, shapes, and degrees of addition are accessible for analysis. Therefore, only averaging information can be obtained, which requires the development/application of techniques for data acquisition founded on a broad statistical basis. Along these lines, we have recently introduced scanning Raman spectroscopy (SRS) and scanning Raman microscopy (SRM) as versatile techniques for a reliable and reproducible characterization of covalently functionalized SCA bulk samples.[3f,g] Despite these improvements, there are still fundamental questions that have not been addressed or solved so far: 1) the exact quantification of the degree of addition of a specific functional entity and 2) a direct comparison of the reactivity of different SCAs under equivalent reaction conditions. Herein, we provide a profound answer for these two fundamental challenges. Based on a novel and versatile reductive arylation of graphite/graphene and carbon nanotubes—utilizing λ^3-iodane precursors—the degree of functionalization has been quantified by a thermogravimetric product analysis, coupled with gas-chromatographic separation and mass-spectrometric characterization (TG-GC-MS). With this setup, we are now able to separate the thermally detached functional entities and to selectively identify and quantify each individual component attached to the carbon allotrope framework.

Results and Discussion

For the λ^3-iodane-based reductive arylation, the respective SCA was initially reduced with a stoichiometric amount of potassium yielding the corresponding nanotubide and graphenide salts,[7] which represent highly activated intermediates. We have recently shown that the stoichiometry of potassium is a critical factor to fine tune the degree of addition in the final single-wall carbon nanotube (SWCNT) derivatives.[8] Therefore, the investigation of the reaction of nanotubides and graphenides with different λ^3-iodanes was carried out by the variation of the potassium/carbon ratio ($T_{(1:4)}$, $T_{(1:8)}$, $T_{(1:16)}$, and $T_{(1:24)}$ as well as $G_{(1:4)}$, $G_{(1:8)}$, $G_{(1:16)}$, and $G_{(1:24)}$ exhibiting a respective carbon to potassium ration of 1:4, 1:8, 1:16, and 1:24) (Scheme 1).

Hypervalent iodine compounds easily form radicals and can be used as functional-group transfer reagents.[9] In the SCA chemistry they have so far only been applied for the electrochemical functionalization of carbon electrodes[10] as well as other types of surfaces.[11] In line with the radical mechanisms

---

[a] F. Hof, R. A. Schäfer, C. Weiss, Dr. F. Hauke, Prof. Dr. A. Hirsch
Department of Chemistry and Pharmacy
and Institute of Advanced Materials and Processes (ZMP)
Friedrich-Alexander-Universität Erlangen–Nürnberg (FAU)
Henkestrasse 42, 91054 Erlangen (Germany)
Fax: (+49) 9131-85-26864
E-mail: andreas.hirsch@fau.de

Supporting information for this article is available on the WWW under http://dx.doi.org/10.1002/chem.201404662.

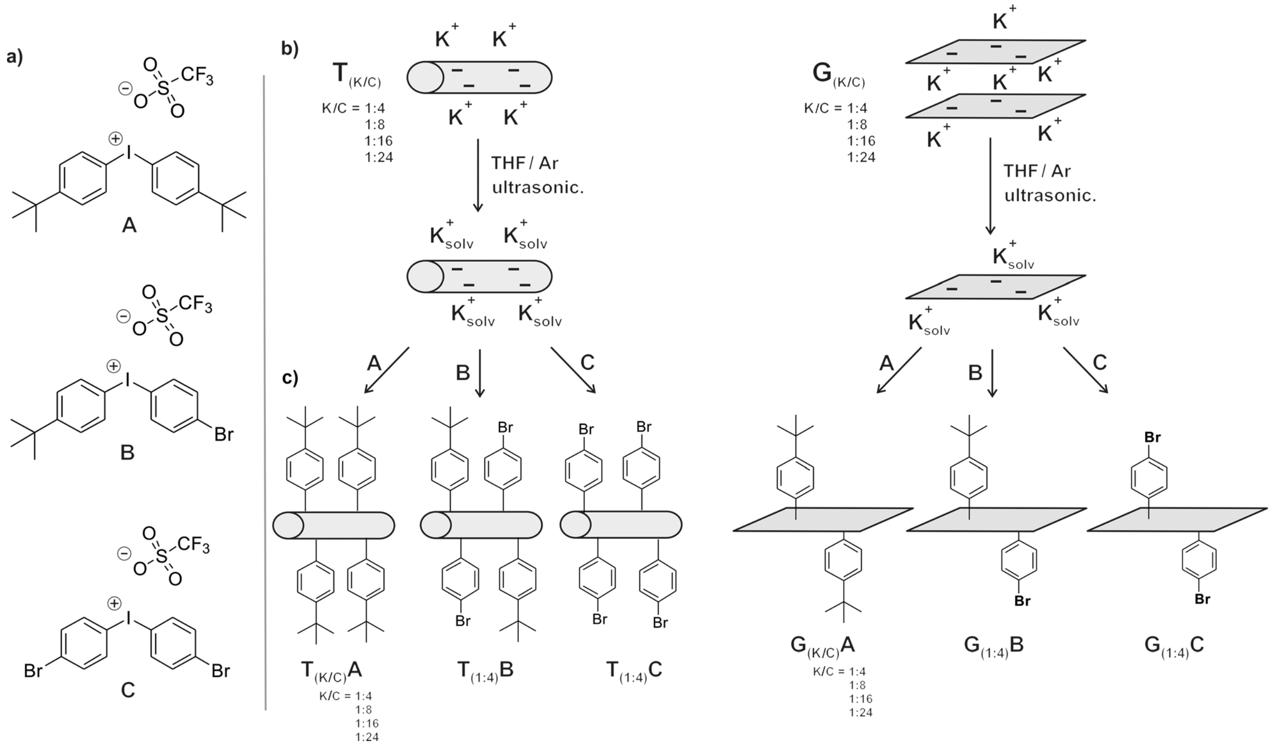

Scheme 1. a) Diaryliodonium triflates A, B and C. b) Reductive activation and dispersion of SWCNTs/graphite with variation of the potassium concentration. c) Covalent functionalization of negatively charged carbon intermediates with λ^3-iodanes.

stated for reductive arylation/alkylation reactions and diazonium-based SCA functionalizations,[12] an equivalent pathway can be anticipated for the reaction of λ^3-iodanes. In order to screen their reactivity as SCA trapping electrophiles, three different *para*-functionalized λ^3-iodanes, that is, bis-(4-(*tert*-butyl)phenyl) iodonium trifluoromethane-sulfonate (A), (4-bromophenyl)(4-(*tert*-butyl)phenyl iodonium trifluoro-methanesulfonate (B), and bis-(4-bromophenyl) iodonium trifluoro-methanesulfonate (C), have been synthesized by adjusting literature-known procedures (for details see the Supporting Information).[13] For the synthesis of the arylated SCA derivatives, the corresponding potassium nanotubide/graphenide salt was dispersed in THF_{abs} (glovebox: Ar) and subsequently 0.5 equivalents per carbon of the respective λ^3-iodane A–C were added. The isolation of the reaction products T(A–C) and G(A–C) was accomplished by aqueous workup and filtration. In order to gain statistically significant bulk information about the success of this covalent functionalization pathway scanning Raman spectroscopy was carried out. Here, the $I_{(D/G)}$ (intensity ratio of the D- and G-bands) values of the individual Raman spectra (at least 1.250 single-point spectra measured) are plotted with respect to their frequency and the respective distribution function was determined (Figure 1).

In principle, the D-band intensity is a measure for the amount of lattice sp^3 centers introduced by covalent addend binding. The successful reaction of the reduced SCAs with the λ^3-iodanes A–C can exemplarily be demonstrated (K/C = 1:4) on the basis of the Raman data of the functionalized SWCNTs ($\lambda_{exc} = 633$ nm, Figure 1, top) and the graphite/graphene[14] derivatives ($\lambda_{exc} = 532$ nm, Figure 1, bottom) (see also Table 1). For further Raman data see Figures S1 and S2 in the Supporting Information.

Table 1. Statistical Raman spectroscopic data of the reaction products $T_{(1:n)}$(A–C) and $G_{(1:n)}$(A–C)—$I_{(D/G)}$ values with standard deviation Δ.

SWCNT	$I_{(D/G)}$ (λ=633 nm)	Δ	Graphite/graphene	$I_{(D/G)}$ (λ=532 nm)	Δ
$T_{(1:4)}A$	0.95	0.15	$G_{(1:4)}A$	1.00	0.30
$T_{(1:4)}B$	0.90	0.11	$G_{(1:4)}B$	1.05	0.30
$T_{(1:4)}C$	0.93	0.17	$G_{(1:4)}C$	0.95	0.30
$T_{(1:8)}A$	0.68	0.17	$G_{(1:8)}A$	1.25	0.11
$T_{(1:16)}A$	0.42	0.24	$G_{(1:16)}A$	1.05	0.30
$T_{(1:24)}A$	0.26	0.09	$G_{(1:24)}A$	0.81	0.47

The potential of this novel synthetic route becomes apparent, when the respective $I_{(D/G)}$ values of the carbon nanotube samples $T_{(1:4)}$(A–C) are compared with reference samples prepared by literature-known synthetic pathways obtained by reductive hexylation $T_{(1:4)}$Hex-I or reductive arylation $T_{(1:4)}$Ph-I of carbon nanotubes[15] (see Figure 2).

For arylated SWCNT derivatives accessible by our novel λ^3-iodane-based functionalization sequence, the degrees of functional group addition, represented by the respective RDIs, drastically exceed the values obtained for systems synthesized by classical pathways:[15] for example, RDI($T_{(1:4)}$A) = 1.83 versus RDI($T_{(1:4)}$Ph-I) = 0.83. In accordance with our latest results[8] we also observe a pronounced dependence of the Raman derived

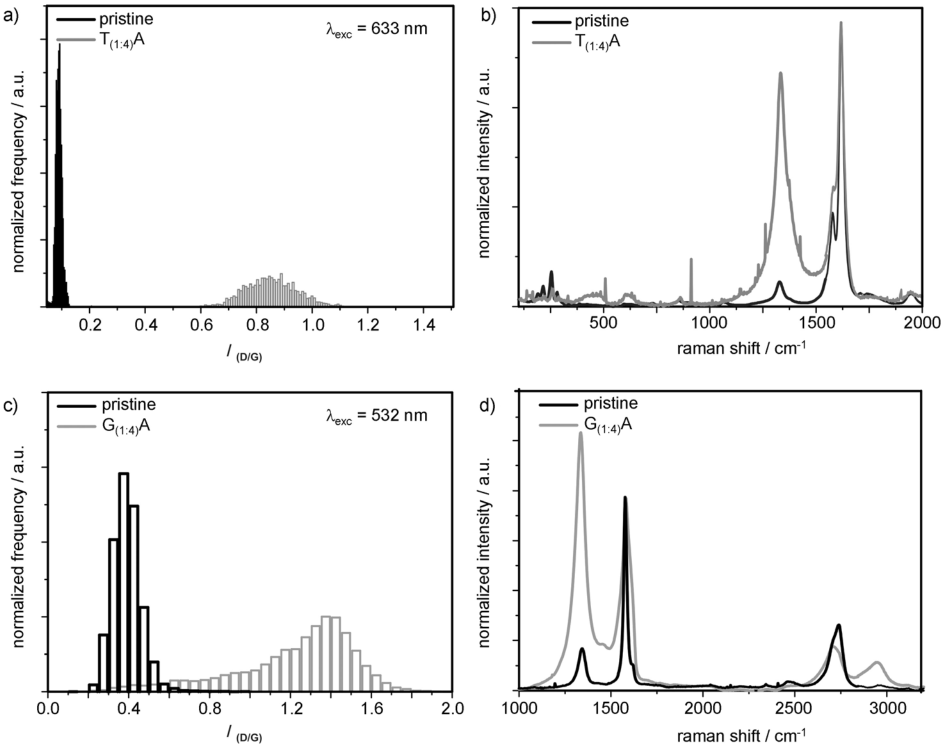

Figure 1. Statistical Raman spectroscopic analysis of the functionalized carbon allotrope $T_{(1:4)}A$ (λ_{exc} = 633 nm) and $G_{(1:4)}A$ (λ_{exc} = 532 nm). a) Histogram and b) mean spectrum of $T_{(1:4)}A$. c) Histogram and d) mean spectrum of $G_{(1:4)}A$.

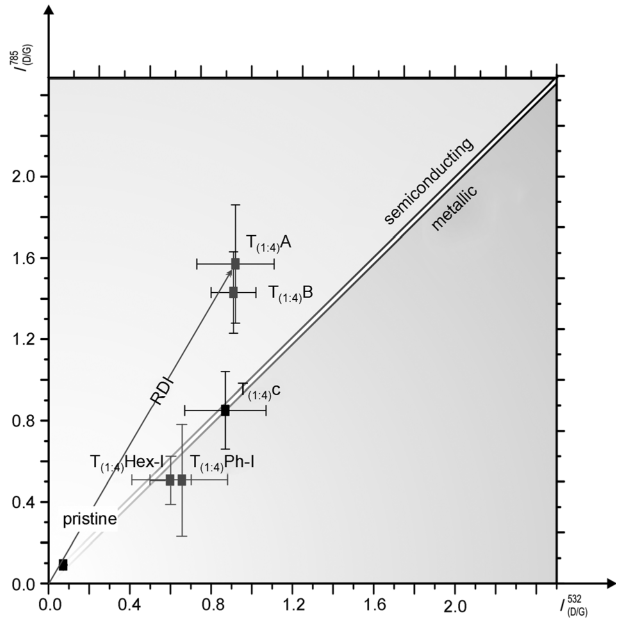

Figure 2. 2D Raman index plot based on the statistical Raman analysis of $T_{(1:4)}A$, $T_{(1:4)}B$, $T_{(1:4)}C$, and the alkylated and arylated reference samples $T_{(1:4)}$Hex-I and $T_{(1:4)}$Ph-I. The respective values for the Raman defect index (RDI), the Raman homogeneity index (RHI), and the Raman selectivity index (RSI) are summarized in Figure S3 in the Supporting Information.

$I_{(D/G)}$ value on the amount of potassium used for the reduction for the SWCNT samples and for the graphite/graphene samples (Figures S4–S6 in the Supporting Information; Table 1). The final degree of functionalization increases with the respective amount of potassium used in the reductive SCA activation step.

Furthermore, we were able to show that these covalently bound aryl moieties can reversibly be detached from the carbon allotrope framework either by laser-induced de-functionalization (exemplarily shown for $T_{(4:1)}A$; λ_{exc} = 785 nm, E = 10 mW, Figure 3, left, Figure S7 in the Supporting Information) or thermally. The latter approach opens the possibility to monitor the detachment progress of the functional moieties directly by Raman spectroscopy (Figure 2, right, Figure S8 in the Supporting Information).

Here, for both functionalized SCA derivatives—$T_{(1:4)}A$ and $G_{(1:4)}A$—a continuous decrease of the D-band intensity is observed starting from around 150 °C up to 500 °C. At temperatures around 500 °C, the characteristic Raman spectrum of the respective starting material is restored exhibiting an $I_{(D/G)}$ value of less than 0.1 in the bulk (Figure S8 in the Supporting Information). However, neither by SRS nor by temperature-depending Raman spectroscopy any conclusion about the chemical nature of the attached moieties can be extracted. Thus, thermogravimetric analysis coupled to mass spectrometry (TG-MS) was carried out (20–700 °C, constant flow of N_2 (70 mL min^{-1}, Figures S9–S14 in the Supporting Information). In the region between 20 and 130 °C, mainly physisorbed THF and water is released from the samples $T_{(1:4)}$(A–C). According to the respective mass traces, sample mass loss beyond 500 °C mainly can be traced back to the degradation of the carbon framework. The predominant mass loss of 23.2 ($T_{(1:4)}A$), 17.9 ($T_{(1:4)}B$), and 28.0 % ($T_{(1:4)}C$) is detected between 130 and 500 °C and nicely correlates with the respective flux of the detected ion currents, which are the characteristic fragments originating from the detached *tert*-butylbenzene and/or bromobenzene moieties (Figures S9–S11 in the Supporting Information). The same consistent data set was obtained for the functionalized graphite/graphene derivatives $G_{(1:4)}$(A–C). However, in this case the observed overall mass loss is considerably lower: 5.4 ($G_{(1:4)}A$), 10.5 ($G_{(1:4)}B$), and 3.2 % ($G_{(1:4)}C$) (see Figures S12–S14 in the Supporting Information). The TG-MS-based data nicely corroborates the Raman results regarding an efficient covalent addend binding in both carbon allotropes. Nevertheless, up to now it was not possible to determine an exact value of the degree of the functionalization of covalently modified SCAs as Raman spectroscopy only allows to draw information about the amount of

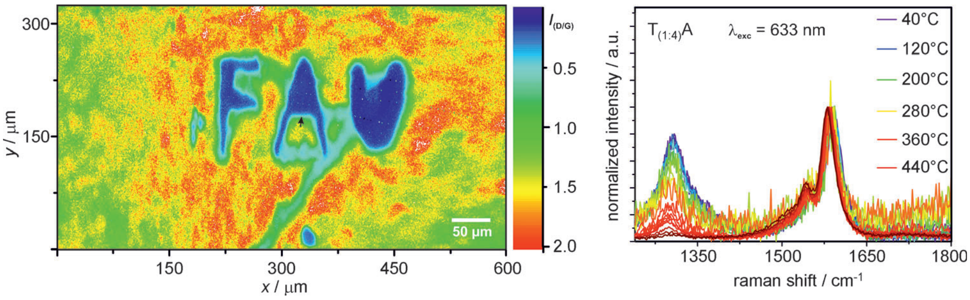

Figure 3. Left: Laser-induced thermal de-functionalization of the functionalized bulk material $T_{(1:4)}A$ demonstrating the reversibility of addend binding. Regions in blue color denote areas with lower degrees of functionalization based on a thermal de-functionalization by "writing" with high laser power. Right: Temperature-dependent Raman spectroscopy of *tert*-butylphenyl-functionalized SWCNTs ($\lambda_{exc} = 633$ nm).

symmetry breaking defects in the sp^2 carbon lattice and thermogravimetric measurements provide only information about the overall sample mass loss attributed to a thermal detachment of all physisorbed and chemisorbed species. To circumvent these obstacles we employed thermogravimetric-based, gas chromatography coupled to mass spectrometry (TG-GC-MS, see Figure 4). This allowed us to determine the mass-loss region, where the covalently bound addend is detached—based on this data an exact quantification of the amount of bound functional groups is possible.

For this purpose, 1 mL of the carrier gas was collected at a sample temperature of 250 °C (highest mass flux) and the individual components were separated by a high-performance GC column (Elite-5MS capillary column)—temperature gradient: 10 K min^{-1}, $T = 40–240$ °C. Subsequently, the respective sample fractions were analyzed by mass spectrometry. The corresponding retention times are depicted in Figure 4, right. Here, the bromophenyl moiety of $T_{(1:4)}B$ and $T_{(1:4)}C$ is detected at a retention time of 4.93 min, whereas the *tert*-butylphenyl addend in $T_{(1:4)}A$ and $T_{(1:4)}B$ is detected at a retention time of 5.84 min (MS fragmentation pattern: see Figure S15 in the Supporting Information). In the mixed functionalized systems $T_{(1:4)}B/G_{(1:4)}B$ both thermally detached functional moieties can be identified, exhibiting a peak area ratio of almost 1:1 (Figures S16 and S17 in the Supporting Information).

This result clearly highlights the potential and versatility of our novel functionalization sequence. Starting from an easily accessible λ^3-iodane precursor system with two different aryl moieties, carbon-allotrope-based architectures with complementary functional groups—like for instance donor/acceptor systems—can be built up in an one-pot synthesis.

Next to the identification of the main components by TG-GC-MS, formation of byproducts can also be investigated by this setup. Here, in all three functionalized SWCNT samples (Figure S16 in the Supporting Information), additional components (below 3 % total peak area) are detected by GC (retention time of 1.93, 1.95, and 2.04 min), which can be attributed to THF (solvent) and degradation products thereof (furane, dihydrofurane). Remarkably, in the case of the graphite/graphene adducts $G_{(1:4)}(A–C)$ the peak for THF (retention time of 2.04 min) is observed as main component (≈80 %) (Figure S17 in the Supporting Information). Moreover, in direct comparison, the peak area of the detached *tert*-butylphenyl moieties for the SWCNT derivatives $T_{(1:4)}A$ and $T_{(1:4)}B$ is by two orders of magnitude higher than that detected for the corresponding graphite/graphene adducts $G_{(1:4)}A$ and $G_{(1:4)}B$. Apparently, the degree of covalent functionalization is considerably higher for carbon nanotubes. These results can be attributed to the fact that in the case of graphite, the reduction and dispersing steps do not exclusively yield completely exfoliated and individualized graphene sheets. The detection of THF as major component is likely to be traced back to intercalated solvent molecules, which are trapped between the carbon sheets. This also reduces the accessible carbon surface area for the hypervalent

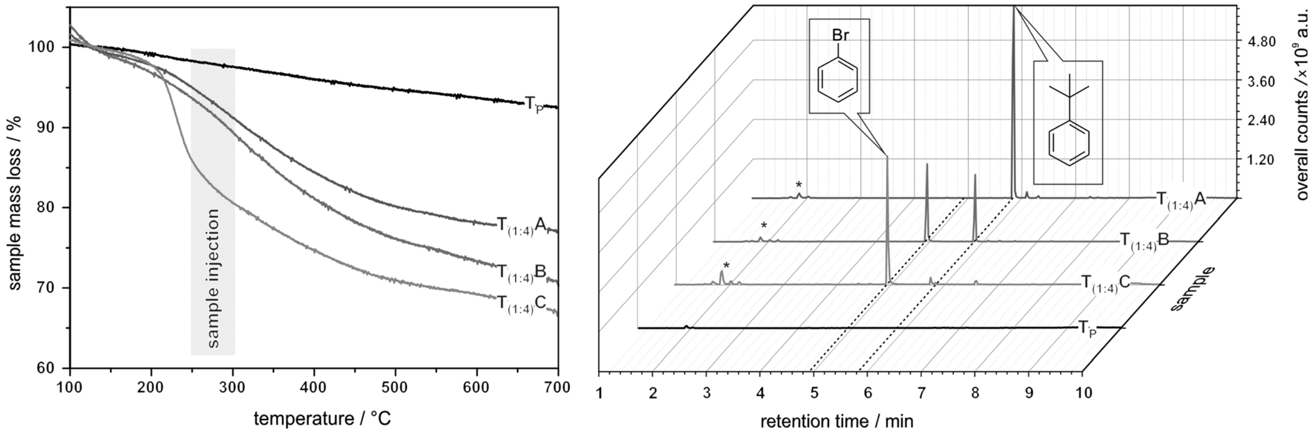

Figure 4. TG-GC-MS analysis of the functionalized SWCNT samples $T_{(1:4)}A$, $T_{(1:4)}B$, and $T_{(1:4)}C$. Left: Plot of mass loss versus the temperature. Right: GC-MS analysis of 1 mL gaseous addends detached at 250 °C.

iodine compounds, which decreases the overall degree of functionalization and yields an explanation for the high amount of THF in the TG-GC-MS experiments. This rationale could be corroborated by a reference experiment where a graphite starting material with initial smaller flake size was chosen. Here, only a negligible amount of THF in relation to the *tert*-butylphenyl signal is observed by GC (Figure S18 in the Supporting Information).

In order to confirm that the obtained GC-MS traces originate from covalently bound functional groups and not from intercalated λ^3-iodanes, we carried out an additional reference experiment where the hypervalent iodine compound B was blended with graphite (Figure 5). The GC elugram of the reference sample differs distinctively from the elugrams of the covalently functionalized SCA derivatives as it contains not only the characteristic fragmentation pattern of the *tert*-butyl- and bromophenyl groups, but also several other compounds originating from the trifluoromethyl sulfonate counter ion of the λ^3-iodane B (not found for covalently functionalized samples).

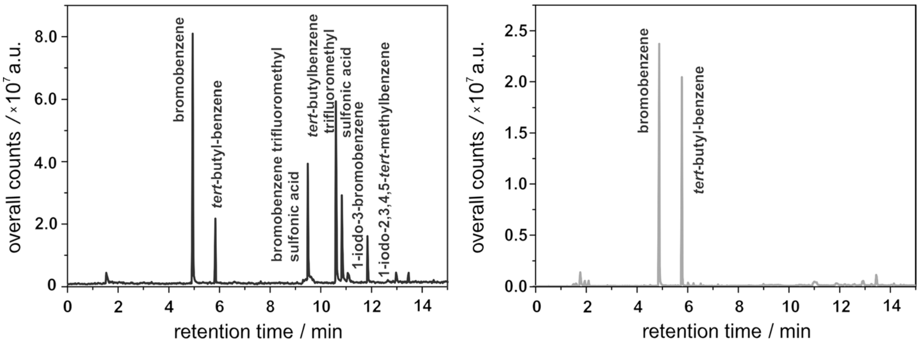

Figure 5. Reference experiment—graphite/λ^3-iodane blend. Left: Elugram of the pristine λ^3-iodane B (TTG = 230 °C) thermal fragmentation products. The mass-spectrometric-identified compounds are attributed to the respective retention times of 4.93, 5.84, 9.51, 10.62, 10.85, and 11.86 min. Right: For comparison—elugram of the covalently functionalized SWCNT derivative $T_{(1:4)}B$.

The separation of thermally detached functional moieties and the identification of their chemical identity is a fundamental advantage provided by the TG-GC-MS setup. This fact is also nicely illustrated by the characterization of an *n*-hexyl-functionalized SWCNT reference sample (Figure S19 in the Supporting Information). Here, besides *n*-hexane as main component, characteristic byproducts[8] like hexanol, hexanal, and hexyliodide are also individually separated by GC and identified by MS. These results nicely confirm our published data concerning the multifunctional product distribution of reductively functionalized SWCNT samples and highlight the demand of powerful analytical techniques for their investigation. Nevertheless, for an exact determination of the amount of covalently attached addends a reliable calibration for the TG-GC-MS-based analysis is a fundamental prerequisite. For this purpose, we systematically varied the amount of $T_{(1:4)}A$ and $G_{(1:4)}A$ (Figures S20 and S21 in the Supporting Information). As the detachment of the addends takes place mainly in the temperature regime between 130 and 500 °C, the detected overall mass loss in this region was weighed by the percentage of the peak area of the corresponding *tert*-butylbenzene detached from the respective SCA (0.95 for $T_{(1:4)}A$ and 0.16 for $G_{(1:4)}A$) (Figure S22 in the Supporting Information). For each thermogravimetric experiment the corresponding amounts of *tert*-butylbenzene were extracted (Figure S23 in the Supporting Information) and were correlated to the peak area of the GC-MS elugram by using different weight portions of samples during the thermogravimetric analysis of the specified samples versus the integrated peak area of the GC-MS trace. The linear fit (Figure 6) yields the pre-factor $(3.24 \pm 0.14)\times10^{-11}$ (standard deviation: 4 %) and provides the basis for the direct quantification of the functional groups attached to carbon nanotubes as well as to graphene/graphite. On the basis of the experimentally determined calibration factor, the amount of *tert*-butylbenzene in the mixed-functionalized samples $T_{(1:4)}B$ and $G_{(1:4)}B$ can be calculated as 1.98 and 0.01 µmol, respectively. According to the detected 1:1 ratio of the peak areas (*tert*-butylbenzene/bromobenzene) it is furthermore possible to quantify the amount of the detached bromobenzene groups in $T_{(1:4)}B$ (2.03 µmol) and $T_{(1:4)}C$ (3.25 µmol) (Figure S16 in the Supporting Information). An amount of 0.010 µmol was found for $G_{(1:4)}B$ and of 0.026 µmol for $G_{(1:4)}C$ (Figure S17 in the Supporting Information).

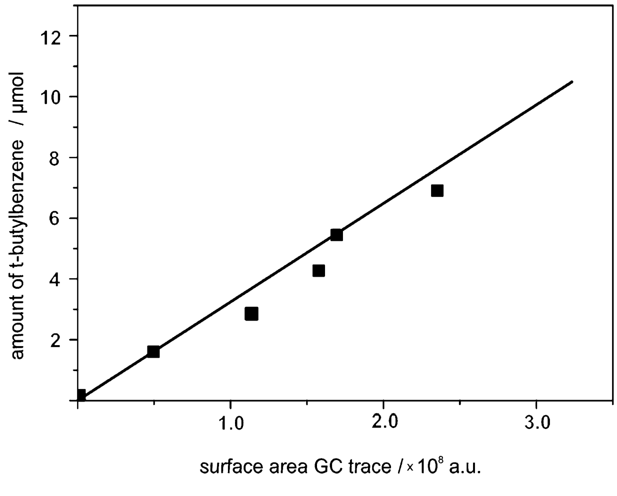

Figure 6. TG-GC-MS calibration curve by using different sample weights (0.5–8.3 mg) of $T_{(1:4)}A$ and $G_{(1:4)}B$ (■, —— = linear fit) during the thermogravimetric analysis. $R^2 = 0.9835$, $\Delta x = (3.24 \pm 0.14)\times10^{-11}$.

Furthermore, the amount of potassium used in the SCA activation step (Figures S24 and S25 in the Supporting Information) can be correlated with the final amount of attached functional moieties. The respective data is collected in Table ST2 in the Supporting Information.

For the first time it is now possible to exactly quantify the degree of functionalization (*f*-addends in relation to SCA lattice carbon atoms, Table 2) of a given functionalization sequence, as the region of mass loss attributed to the functional-group detachment is identified by TG-MS and the amount of a specific covalently bound addend is determined by TG-GC-MS. This is the advantage of this setup as contributions of side products, solvent residues, and sample impurities can be identified and the detected sample mass loss, used for the calculation of the degree of functionalization, can exactly be assigned to the specific functional entity of interest.

Table 2. Correlation of the amount of attached functional addends with the amount of lattice carbon atoms in the respective functionalized SCA derivatives.

SWCNT	*f*-Addend per lattice carbon [%]	Graphite/graphene	*f*-Addend per lattice carbon [%]
$T_{(1:4)}A$	3.42	$G_{(1:4)}A$	0.04
$T_{(1:4)}B$	2.51	$G_{(1:4)}B$	0.02
$T_{(1:4)}C$	2.02	$G_{(1:4)}C$	0.01
$T_{(1:8)}A$	2.45	$G_{(1:8)}A$	0.13
$T_{(1:16)}A$	0.80	$G_{1:16)}A$	0.04
$T_{(1:24)}A$	0.25	$G_{(1:24)}A$	0.02

Apparently, the TG-GC-MS-determined degrees of addition in the respective SCA derivatives (Figures S24 and S25 in the Supporting Information) nicely correlate with the development of the $I_{(D/G)}$ values, discussed above. To demonstrate that the reductive activation with potassium is indeed crucial for the covalent functionalization with λ^3-iodanes, reference experiments with pristine carbon nanotubes and graphite starting materials have been carried out under various experimental conditions: 1) stirring at RT (4 h), 2) stirring under light irradiation (4 h), and 3) stirring under heating to reflux (4 h). The respective samples have been investigated by Raman spectroscopy and TG-MS (Figures S26–S29 in the Supporting Information). In contrast to the measured $I_{(D/G)}$ values for the reductively activated SCAs (0.95 for $T_{(1:4)}A$, 1.00 for $G_{(1:4)}A$) only a negligible increase of the $I_{(D/G)}$ value (Figures S26 and S28 in the Supporting Information) in relation to the pristine starting allotrope was detected for all three reference experiments. These findings are also corroborated by the corresponding TG-MS data (Figures S27 and S29 in the Supporting Information).

These results nicely illustrate the important role of reductively activated SCA intermediates for the covalent functionalization of carbon allotropes. Together with a suitable electrophile—here λ^3-iodanes—functional entities can very efficiently be grafted onto the SCA framework. Dyke et al.[12a] as well as Chattopadhyay et al.[12b] have shown that these types of reductive functionalization sequences are based on single-electron transfer processes from the charged carbon allotrope intermediates towards the trapping electrophile. This leads directly to the formation of highly reactive radical species in close proximity to the SCA carbon framework and subsequently, the trapping electrophile is covalently bound. As mentioned above, hypervalent iodine compounds can easily form radicals and therefore a similar radical mechanism can be anticipated for our novel λ^3-iodane-based functionalization route. First evidence for this assumption was obtained from a GC-MS-based byproduct analysis. Here, the organic components in the solvent phase, obtained after the aqueous workup of the primary reaction mixture—λ^3-iodane C, were separated by GC and identified by mass spectrometry. Besides 1-bromo-4-iodobenzene as main component, biphenyl derivatives as characteristic radical recombination products were detected (Figure S30 in the Supporting Information).

Conclusion

In conclusion, we have introduced a new λ^3-iodane-based reaction sequence as a versatile and efficient tool for the functionalization of reductively exfoliated and activated SCAs. The covalent aryl binding can be confirmed by SRS and SRM as well as by TG-MS studies. By the aid of temperature-dependent Raman investigations it can be shown that the introduced functional moieties can reversibly be detached in a temperature region up to 480 °C. This information provided the basis for TG-GC-MS coupling experiments where it was shown that the thermally detached entities can be identified by MS as one major component after GC separation. These findings enabled us to quantify the amount of covalently bound aryl functionalities, allowing us to exactly calculate the percentage of functionalized carbon atoms for each individual component.

Experimental Section

Materials

Purified HiPco SWCNTs (grade: pure; lot number P0261, TGA residue 13.3 % wt) were purchased from Unidym Inc. (Sunnyvale, CA) and were used without further treatment. Synthetic spherical graphite (SGN18, 99.99 % C, TGA residue 0.01 % wt—Future Carbon, Germany) with a mean grain size of 18 μm and a specific surface area of 6.2 $m^2 g^{-1}$ was used after annealing under vacuum (300 °C).

Chemicals and solvents were purchased from Sigma Aldrich Co. (Germany) and were used as-received if not stated otherwise.

THF was distilled three times under an argon inert gas atmosphere in order to remove residual water: 1) over CaH_2, 2) over sodium, and 3) over sodium–potassium alloy. Residual traces of oxygen were removed by pump freeze treatment (three iterative steps). THF_{abs} was used for all reactions.

Glovebox

Sample functionalization was carried out in an argon-filled Labmaster sp glovebox (MBraun), equipped with a gas filter to remove solvents and an argon cooling systems, with an oxygen content <0.1 ppm and a water content <0.1 ppm.

Raman spectroscopy

Raman spectroscopic characterization was carried out on a Horiba-LabRAM Aramis confocal Raman microscope ($\lambda_{exc}=532$, 633, 785 nm) with a laser spot size of about 1 μm (Olympus LMPlanFl 100×, NA 0.80). The incident laser power was kept as low as possible to avoid structural sample damage: 127 μW (532 nm) for SWCNT samples or 1.35 mW (532 nm) for graphite samples, 36 μW (633 nm) and 100 μW (785 nm). Spectra were obtained with a CCD array at −70 °C—grating: 600 grooves per mm (532 and 633 nm) and a 300 groove per mm (785 nm). Spectra were obtained from a 50 μm×50 μm area for SWCNTs or 100×100 μm area for graphite with 2 μm step size in the SWIFT mode for low integration times. Sample movement was carried out by an automated XY-scanning table.

Temperature-depending Raman measurements were performed in a Linkam stage THMS 600, equipped with a liquid nitrogen pump TMS94 for temperature stabilization under a constant flow of nitrogen. The measurements were carried out on Si/SiO_2 substrates (300 nm oxide layer) with a heating rate of 10 $K\,min^{-1}$.

Thermogravimetric analysis (TG) combined with gas-chromatographic separation (GC) coupled with a mass spectrometer (MS)

Thermogravimetric analysis was carried out on a PerkinElmer Pyris 1 TGA instrument. Time-dependent temperature profiles in the range of 20 and 700 °C (20 $K\,min^{-1}$ gradient) were recorded under a constant flow of N_2 (70 $mL\,min^{-1}$). About 2.0 mg initial sample mass were used if not stated otherwise. The evolved gases detached from the respective sample in combination with the N_2 carrier gas is transferred into the GC system through a TL9000 TG-IR-GC interface at a constant temperature of 280 °C. The gas-chromatographic separation was achieved by a GC-Clarus 680 with a polysiloxane-coated Elite-5MS capillary column: 30 m length, 0.25 mm diameter, 0.25 μm film thickness. A GC injection fraction of 1 mL was collected at the respective TG temperature: SWCNT samples (250 °C), graphite samples (300 °C).GC parameters: injector zone = 280 °C, detection zone = 250 °C, split = 8.2 $mL\,min^{-1}$, flow rate helium = 10 $mL\,min^{-1}$, temperature profile = 34 min total run time, dynamic ramp = 24 min, 40–280 °C with a10 $K\,min^{-1}$ gradient followed by an isothermal step of 10 min at 280 °C.

Online MS measurements without GC-separation were carried out with a GC-Clarus 680 with an Elite-5MS glass capillary column: 30 m length, 0.25 mm diameter. GC parameters: injector zone = 280 °C, detection zone = 250 °C, split = 22.6 $mL\,min^{-1}$, flow rate helium = 10 $mL\,min^{-1}$, isothermal temperature profile = 34 min at 280 °C. MS measurements were performed on a MS Clarus SQ8C (multiplier: 1800 V). The obtained data was processed with the TurboMass Software and Bibliograpic searches where performed with NIST MS Search 2.0.

^1H, ^{13}C and ^{19}F NMR spectroscopy

NMR spectra were recorded on a Jeol JNM EX 400 (400 MHz for ^1H and 100 MHz for ^{13}C) and a Bruker Avance 300 (300 MHz for ^1H, 75 MHz for ^{13}C and 282 MHz for ^{19}F) spectrometer. Chemical shifts are reported in [ppm] at room temperature. Abbreviations used for splitting patterns are: s = singlet, d = doublet, t = triplet, m = multiplet.

Synthesis of the λ^3-iodanes

The syntheses of the λ^3-iodanes were adapted from the work of B. Olofsson and her research group.[13a] *m*-Chloroperbenzoic acid was dried under reduced pressure before use. Dichloromethane was distilled once under reduced pressure before use.

Synthesis of *f*-SCA

Carbon nanotubide salts with varying potassium/carbon ratios: $T_{(1:4)}$ (K/C=1:4)], $T_{(1:8)}$ (K/C=1:8), $T_{(1:16)}$ (K/C=1:16), $T_{(1:24)}$ (K/C=1:24): In an argon-filled glovebox (<0.1 ppm oxygen, <0.1 ppm H_2O), HiPco SWCNTs (12.00 mg, 1.000 mmol) and the respective amount of potassium—$T_{(1:4)}$ (9.775 mg, 0.250 mmol, K/C = 1:4), $T_{(1:8)}$ (4.887 mg, 0.125 mmol, K/C = 1:8), $T_{(1:16)}$ (2.444 mg, 0.063 mmol, K/C = 1:16), $T_{(1:24)}$ (1.667 mg, 0.042 mmol, K/C = 1:24)—were heated under stirring at 150 °C for 8 h. Afterwards, the respective salt was allowed to cool to RT and isolated as a black (K/C = 1:24, 1:16, and 1:8) or beige (K/C = 1:4) material.

Graphite intercalation compounds with varying potassium/carbon ratios: $G_{(1:4)}$ (K/C=1:4), $G_{(1:8)}$ (K/C=1:8), $G_{(1:16)}$ (K/C=1:16), $G_{(1:24)}$ (K/C=1:24): In an argon-filled glovebox (<0.1 ppm oxygen, <0.1 ppm H_2O), spherical graphite (SGN18) (12.00 mg, 1.000 mmol) and the respective amount of potassium—$G_{(1:4)}$ (9.775 mg, 0.250 mmol, K/C = 1:4), $G_{(1:8)}$ (4.887 mg, 0.125 mmol, K/C = 1:8), $G_{(1:16)}$ (2.444 mg, 0.063 mmol, K/C = 1:16), $G_{(1:24)}$ (1.667 mg, 0.042 mmol, K/C = 1:24)—were heated under stirring at 150 °C for 8 h. Afterwards, the respective salt was allowed to cool to RT and isolated as a black (K/C = 1:24), bronze (K/C = 1:16 and 1:8), or beige (K/C = 1:4) material.

SWCNT: λ^3-iodane variation—preparation of $T_{(1:4)}$A, $T_{(1:4)}$B, $T_{(1:4)}$C: In an argon-filled glovebox (<0.1 ppm oxygen, <0.1 ppm H_2O), the carbon nanotubide salt $T_{(1:4)}$ (21.7 mg salt, 1 mmol carbon) and the corresponding λ^3-iodane—A (293 mg, 0.50 mmol), B (265 mg, 0.50 mmol), or C (238 mg, 0.50 mmol)—were dispersed by the addition of THF_{abs} (20 mL, three different 50 mL round bottom flasks) and by the aid of a 5 min tip ultrasonication treatment step (Bandelin UW 3200, 600 $J\,min^{-1}$). The respective dispersion ($T_{(1:4)}$A, $T_{(1:4)}$B, $T_{(1:4)}$C) was stirred for 14 h. Afterwards, the reaction mixture was transferred from the glovebox and water (50 mL) and a few drops of HCl (until pH 4 is reached) were added to the dispersion. The reaction mixture was transferred to a separation funnel with cyclohexane (50 mL). The phases were separated and the organic layer, containing the functionalized SWCNT material, was purged three times with distilled water. The organic layer was filtered through a 0.2 μm reinforced cellulose membrane filter (Sartorius) and washed THF (3×100 mL). The covalently functionalized SWCNTs were scraped off the filter paper and the material was dried in vacuum.

Graphene: λ^3-iodane variation—preparation of $G_{(1:4)}$A, $G_{(1:4)}$B, $G_{(1:4)}$C: In an argon-filled glovebox (<0.1 ppm oxygen, <0.1 ppm H_2O), the graphite intercalation compound $G_{(1:4)}$ (21.7 mg, 1 mmol carbon) and the corresponding λ^3-iodane—A (293 mg, 0.50 mmol), B (265 mg, 0.50 mmol), or C (238 mg, 0.50 mmol)—were dispersed by the addition of THF_{abs} (20 mL, three different 50 mL round bottom flasks) and by the aid of a 5 min tip ultrasonication treatment step (Bandelin UW 3200, 600 $J\,min^{-1}$). The respective dispersion ($G_{(1:4)}$A, $G_{(1:4)}$B, $G_{(1:4)}$C) was stirred for 14 h. Afterwards, the reaction mixture was transferred from the glovebox and water (50 mL) and a few drops of HCl (until pH 4 is reached) were added to the dispersion. The reaction mixture was transferred to a separation funnel with cyclohexane (50 mL). The phases were separated and the organic layer, containing the functionalized material, was purged three times with distilled water. The organic layer was filtered through a 0.2 μm reinforced cellulose membrane filter (Sartorius) and washed three times with 100 mL of THF. The covalently functionalized material was dried in vacuum.

SWCNT: variation of the potassium/carbon ratio—preparation of $T_{(1:4)}$A, $T_{(1:8)}$A, $T_{(1:16)}$A, $T_{(1:24)}$A: In an argon-filled glovebox (<0.1 ppm oxygen, <0.1 ppm H_2O), the respective carbon nanotubide salt (1 mmol carbon)—$T_{(1:4)}$ (21.7 mg), $T_{(1:8)}$ (16.8 mg), $T_{(1:16)}$ (14.4 mg), $T_{(1:24)}$ (13.7 mg)—and A (293 mg, 0.50 mmol) were dispersed by the addition of THF_{abs} (20 mL, four different 50 mL round bottom flasks) and by the aid of a 5 min tip ultrasonication treatment step (Bandelin UW 3200, 600 J min^{-1}). The respective dispersion ($T_{(1:4)}$A, $T_{(1:8)}$A, $T_{(1:16)}$A, $T_{(1:24)}$A) was stirred for 14 h. Afterwards, the reaction mixture was transferred from the glovebox and water (50 mL) and a few drops of HCl (until pH 4 is reached) were added to the dispersion. The reaction mixture was transferred to a separation funnel with cyclohexane (50 mL). The phases were separated and the organic layer, containing the functionalized SWCNT material, was purged three times with distilled water. The organic layer was filtered through a 0.2 μm reinforced cellulose membrane filter (Sartorius) and washed three times with 100 mL of THF. The covalently functionalized SWCNTs were scraped off the filter paper and the material was dried in vacuum.

Graphene: variation of the potassium/carbon ratio—preparation of $G_{(1:4)}$A, $G_{(1:8)}$A, $G_{(1:16)}$A, $G_{(1:24)}$A: In an argon-filled glovebox (<0.1 ppm oxygen, <0.1 ppm H_2O), the respective graphite intercalation compound (1 mmol carbon)—$G_{(1:4)}$ (21.7 mg), $G_{(1:8)}$ (16.8 mg), $G_{(1:16)}$ (14.4 mg), $G_{(1:24)}$ (13.7 mg)—and A (293 mg, 0.50 mmol) were dispersed by the addition of THF_{abs} (20 mL, four different 50 mL round bottom flasks) and by the aid of a 5 min tip ultrasonication treatment step (Bandelin UW 3200, 600 J min^{-1}). The respective dispersion ($G_{(1:4)}$A, $G_{(1:8)}$A, $G_{(1:16)}$A, $G_{(1:24)}$A) was stirred for 14 h. Afterwards, the samples are removed out of the glovebox and water (50 mL) and a few drops of HCl (until pH 4 is reached) were added to the dispersions. The reaction mixture was transferred to a separation funnel with cyclohexane (50 mL). The phases were separated and the organic layer, containing the functionalized material, was purged three times with distilled water. The organic layer was filtered through a 0.2 μm reinforced cellulose membrane filter (Sartorius) and washed three times with THF (100 mL). The covalently functionalized material was dried in a vacuum.

Acknowledgements

The authors thank the Deutsche Forschungsgemeinschaft (DFG - SFB 953, Project A1 “Synthetic Carbon Allotropes”) and the European Research Council (ERC; grant agreement no. 246622 GRAPHENOCHEM) for financial support. The research leading to these results has received funding from the European Union Seventh Framework Programme under grant agreement no. 604391 Graphene Flagship.

Keywords: analytical chemistry · carbon allotropes · graphene · hypervalent iodine · nanotubes

[1] a) S. Eigler, A. Hirsch, *Angew. Chem.* **2014**, *126*, 7852–7872; *Angew. Chem. Int. Ed.* **2014**, *53*, 7720–7738; b) C. K. Chua, M. Pumera, *Chem. Soc. Rev.* **2013**, *42*, 3222–3233; c) N. Karousis, N. Tagmatarchis, D. Tasis, *Chem. Rev.* **2010**, *110*, 5366–5397; d) A. Hirsch, J. M. Englert, F. Hauke, *Acc. Chem. Res.* **2013**, *46*, 87–96; e) A. Hirsch, *Nat. Mater.* **2010**, *9*, 868–871.

[2] F. Liang, L. B. Alemany, J. M. Beach, W. E. Billups, *J. Am. Chem. Soc.* **2005**, *127*, 13941–13948.

[3] a) G. L. C. Paulus, Q. H. Wang, M. S. Strano, *Acc. Chem. Res.* **2013**, *46*, 160–170; b) S. A. Hodge, M. K. Bayazit, K. S. Coleman, M. S. P. Shaffer, *Chem. Soc. Rev.* **2012**, *41*, 4409–4429; c) M. Quintana, E. Vazquez, M. Prato, *Acc. Chem. Res.* **2013**, *46*, 138–148; d) E. Bekyarova, S. Sarkar, F. Wang, M. E. Itkis, I. Kalinina, X. Tian, R. C. Haddon, *Acc. Chem. Res.* **2013**, *46*, 65–76; e) C. Backes, J. M. Englert, N. Bernhard, F. Hauke, A. Hirsch, *Small* **2010**, *6*, 1968–1973; f) F. Hof, S. Bosch, J. M. Englert, F. Hauke, A. Hirsch, *Angew. Chem.* **2012**, *124*, 11897–11900; *Angew. Chem. Int. Ed.* **2012**, *51*, 11727–11730; g) J. M. Englert, P. Vecera, K. C. Knirsch, R. A. Schäfer, F. Hauke, A. Hirsch, *ACS Nano* **2013**, *7*, 5472–5482.

[4] Z. Syrgiannis, V. La Parola, C. Hadad, M. Lucío, E. Vázquez, F. Giacalone, M. Prato, *Angew. Chem.* **2013**, *125*, 6608–6611; *Angew. Chem. Int. Ed.* **2013**, *52*, 6480–6483.

[5] S. Fujii, T. Enoki, *ACS Nano* **2013**, *7*, 11190–11199.

[6] S. Kundu, W. Xia, W. Busser, M. Becker, D. A. Schmidt, M. Havenith, M. Muhler, *Phys. Chem. Chem. Phys.* **2010**, *12*, 4351–4359.

[7] a) A. Pénicaud, P. Poulin, A. Derré, E. Anglaret, P. Petit, *J. Am. Chem. Soc.* **2004**, *127*, 8–9; b) C. Vallés, C. Drummond, H. Saadaoui, C. A. Furtado, M. He, O. Roubeau, L. Ortolani, M. Monthioux, A. Pénicaud, *J. Am. Chem. Soc.* **2008**, *130*, 15802–15804.

[8] F. Hof, S. Bosch, S. Eigler, F. Hauke, A. Hirsch, *J. Am. Chem. Soc.* **2013**, *135*, 18385–18395.

[9] a) E. A. Merritt, B. Olofsson, *Angew. Chem.* **2009**, *121*, 9214–9234; *Angew. Chem. Int. Ed.* **2009**, *48*, 9052–9070; b) J. Malmgren, S. Santoro, N. Jalalian, F. Himo, B. Olofsson, *Chem. Eur. J.* **2013**, *19*, 10334–10342.

[10] C. K. Chan, T. E. Beechem, T. Ohta, M. T. Brumbach, D. R. Wheeler, K. J. Stevenson, *J. Phys. Chem. C* **2013**, *117*, 12038–12044.

[11] a) C. Fontanesi, C. A. Bortolotti, D. Vanossi, M. Marcaccio, *J. Phys. Chem. A* **2011**, *115*, 11715–11722; b) K. H. Vase, A. H. Holm, K. Norrman, S. U. Pedersen, K. Daasbjerg, *Langmuir* **2007**, *23*, 3786–3793; c) K. H. Vase, A. H. Holm, S. U. Pedersen, K. Daasbjerg, *Langmuir* **2005**, *21*, 8085–8089.

[12] a) C. A. Dyke, J. M. Tour, *Nano Lett.* **2003**, *3*, 1215–1218; b) J. Chattopadhyay, S. Chakraborty, A. Mukherjee, R. Wang, P. S. Engel, W. E. Billups, *J. Phys. Chem. C* **2007**, *111*, 17928–17932.

[13] a) M. Bielawski, B. Olofsson, *Chem. Commun.* **2007**, 2521–2523; b) M. Bielawski, B. Olofsson in *Efficient One-Pot Synthesis of Bis(4-tert-Butylphenyl) Iodonium Triflate*, Wiley, New York, **2009**.

[14] The reductive exfoliation sequences does not exclusively yield monolayer material, which is discussed in the course of the manuscript.

[15] a) F. Liang, A. K. Sadana, A. Peera, J. Chattopadhyay, Z. Gu, R. H. Hauge, W. E. Billups, *Nano Lett.* **2004**, *4*, 1257–1260; b) J. Chattopadhyay, A. K. Sadana, F. Liang, J. M. Beach, Y. Xiao, R. H. Hauge, W. E. Billups, *Org. Lett.* **2005**, *7*, 4067–4069.

Received: July 31, 2014